

Photoionization cross section of helium for photon energies 59–67 eV: The $(sp, 2n +)^1P^o$ Rydberg series of autoionizing resonances

Harry D. Morgan

Department of Physics, University of the District of Columbia, Washington, D.C. 20008

David L. Ederer

Center for Radiation Physics, National Bureau of Standards, Washington, D.C. 20234

(Received 23 June 1983)

The central position of the $2s2p\ ^1P^o$ two-electron resonance of He at $206.21\ \text{\AA}$ has been remeasured using the background continuum of the National Bureau of Standards storage ring facility. In addition, the line-shape parameter q and width Γ of the resonance have also been obtained. We obtained a value of 60.151 ± 0.010 eV for the resonance position, -2.6 ± 0.3 for the line-shape parameter, and 0.038 ± 0.002 eV for the width of the resonance. Our value for the resonance position is in good agreement with the theoretical calculation of 60.145 eV of Bhatia and Temkin and lies within the error budget of the previous experimental measurements of Madden and Codling. Parameter values for the other resonances have also been obtained and are in good agreement with the earlier measurements of Madden and Codling.

I. INTRODUCTION

Helium has been an important test case for many theoretical models^{1–4} because the helium atom provides a unique opportunity to study the correlated motion of two electrons moving in a Coulomb field. The continuum photoabsorption cross section of helium has been investigated in detail over a broad energy range.⁵ The excitation of two-electron autoionizing states of helium and the subsequent analysis⁶ of the asymmetric resonant profile provides another important test of the accuracy of the continuum solutions of the Schrödinger equation for this system. Experimentally, the two-electron excitation states converging to the $n = 2$ levels of the helium ion have been investigated by total absorption spectroscopy⁷ and by photoelectron spectroscopy.⁸ The total absorption cross section profile of the lowest energy resonance converging to $n = 3$ levels of the helium ion,⁹ the partial cross section,¹⁰ and the angular asymmetry parameter⁸ β for the Rydberg series of resonances converging to this limit have also been measured.

In this report we wish to focus on the series of resonances converging to the $n = 2$ levels of the helium ion. Up to the present time, the classical work of Madden and Codling⁷ has been the only experimental measurement of the cross section of this system, from which they extracted the parameters that describe the profiles of these resonances. In addition, these resonances have been extensively studied theoretically by several authors.^{11–18} In a series of papers,^{19–23} Bhatia and Temkin have reported calculations of the resonance energy E_r , the shape parameter q , and the width Γ , of several autoionizing states in helium. Recent calculations of Bhatia and Temkin²⁴ corroborate the experimental values of Madden and Codling except for a small difference in the central position of the $2s2p\ ^1P^o$ resonance. In this paper we describe measurements of the

line-profile parameters of several autoionizing states with a series limit of He^+ ($n = 2$). A major goal of these measurements was to complement the latest calculations of Bhatia and Temkin,²⁴ and provide a photometric evaluation of the cross section of the resonances converging to this limit.

II. EXPERIMENTAL

The experimental apparatus has been described in detail elsewhere.²⁵ Briefly, continuum radiation emitted from the U. S. National Bureau of Standards (NBS) 250-MeV electron synchrotron storage ring (SURF-II) has been employed to provide background radiation in the region below $250\ \text{\AA}$ for the observation of these two-electron excitation states. An absorption cell was placed between an elliptical focusing mirror and the entrance slit of a 3-m grazing incidence monochromator. The cell was a stainless-steel tube 96.40 cm in length, equipped with aluminum windows about $0.1\ \mu\text{m}$ thick at each end. Research grade helium gas, without further purification, was admitted into the system via a variable leak and a flow system was established with an equivalent static pressure of about 0.120 Torr or less. The gas load from the gas cell was handled by two 1000 l/s liquid-helium cryopumps located on separation chambers at either end of the cell. Pressure measurements were made with a capacitance manometer. The 3-m grazing incidence scanning monochromator had a spectral bandpass of $0.072\ \text{\AA}$. The channeltron used to detect uv photons was mounted on a carriage constrained to the Rowland circle and the assembly was driven by a lead screw. Another detector, located near the storage ring, monitored visible radiation and thus the electron current in the storage ring. The signal produced by the visible detector was amplified and used to control the wavelength scan speed. Therefore as the beam

decayed, the scan speed decreased proportionately so that the optical system integrated the uv photon flux over a constant number of electrons per data interval. This eliminated the need to correct the transmission data for the slowly decaying electron beam.

III. DATA ANALYSIS

The experimental atomic cross section, expressed in Mb (1 Mb = 10^{-18} cm²), is given by the relation

$$\sigma = 0.1035(T/p) \ln(I_0/I), \quad (1)$$

where T is the temperature in degrees Kelvin, p is the pressure in Torr, and l is the absorption path length in centimeters. The quantity I_0 denotes the incident intensity without the gas in the cell and I is the detected intensity with gas in the cell. As can be seen from Eq. (1) for absorption cross section measurements, not only a knowledge of the ratio of the incident to transmitted radiation is required, but also the temperature, pressure, and length of the absorbing gas or vapor. For the experimental conditions described here there was little difficulty in determining T , l , and p to an accuracy of about 1%. The accuracy of the intensity ratio I_0/I is primarily determined by the linearity of the detector and the counting statistics. Therefore, the accuracy of σ is determined mainly by the accuracy of $\ln(I_0/I)$.

While it is not especially difficult to make relative measurements of the transmission with a precision of 1%, achieving comparable accuracies in absolute intensities is much more difficult because of sources of systematic errors. The major sources of systematic error are (1) second-order radiation, (2) gas impurities, and (3) scattered radiation. Tests were made to assess the source and magnitude of these systematic errors. It was assumed that second-order radiation is negligible since the 1000-Å aluminum-foil absorption-cell windows should reduce second-order radiation to an undetectable level. As for (2) and (3), impurities in the gas would produce a nonzero value of the cross section at the resonance minimum (assuming the correlation index²⁶ $\rho^2=1$ for helium). The minimum cross section was measured to be zero within experimental error, which is also consistent with the assumption that the sources of systematic error (1)–(3) are negligible. The cross section was measured at a fixed wavelength (200 Å) as a function of pressure. The value of the cross section obtained from the slope of the straight line was equal to 1.24 Mb which can be compared to a value of 1.28 Mb obtained from recent measurements.⁵ The excellent agreement between the value of the cross section with the recent critically evaluated compilation⁵ is further evidence that the sources of systematic error (1)–(3) are negligible. Finally, a plot of $\ln(I_0/I)$ versus pressure was observed to be linear, and pass through the origin, within the uncertainties of the measurements. Nonlinearities in this plot would suggest the presence of scattered and/or second-order radiation. From an assessment of these tests, it is estimated that the values of the absorption cross section are accurate to $\pm 4\%$.

The transmission as a function of wavelength was computed from the intensity $I_0(\lambda)$ recorded without gas and

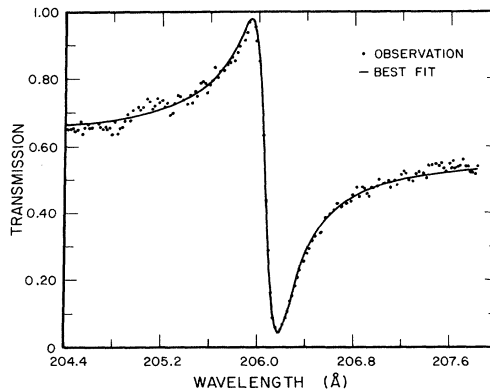


FIG. 1. Typical transmission data for the lowest two-electron excitation state, $2s2p\ ^1P^o$. The data are shown by solid dots; the model transmission calculated from Eqs. (2) and (3) is given by the line.

the intensity $I(\lambda, \sigma, p)$ recorded with gas. The variation of transmission near the lowest $2s2p$ two-electron resonance is shown in Fig. 1 and the transmission for the Rydberg series is shown in Fig. 2. The width of the higher Rydberg series members is comparable to or less than the monochromator bandpass. In order to obtain the undisturbed cross section from the transmission data, it was necessary to deconvolute the cross section from the Gaussian spectrometer window function $W(\lambda)$. This was done by modeling the transmission and comparing it with the experimental data using a nonlinear least-squares fitting algorithm.^{27,28} The model for the transmission is given by

$$I_0(\lambda, q, \Gamma) = \int \exp[-nl\sigma(\lambda', q, \Gamma)] W(\lambda - \lambda') d\lambda', \quad (2)$$

where n , the atom number density, and l , the path length, are measured quantities. The window function $W(\lambda)$ was determined to be Gaussian²⁷ with a full width at half maximum of 0.072 Å. The parameters describing the model cross section were adjusted until a best least-squared fit to the data was obtained.

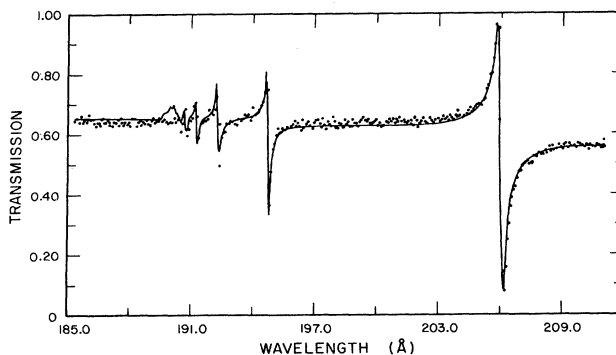


FIG. 2. Transmission profile for the $(sp\ 2n +)\ ^1P^o$ Rydberg series for levels up to $n = 10$. Data are shown by solid dots; the model transmission obtained from Eqs. (2) and (3) is given by the line.

The form of the cross section σ is given by the formalism developed by Fano⁶ for a Rydberg series interacting with one continuum (i.e., $\rho^2=1$). Thus the cross section for the $(sp, 2n+)^1P^o$ Rydberg series can be modeled by the expression

$$\sigma(\lambda, q, \Gamma) = \sigma_b(\lambda) \left[\frac{\left[\sum (q_n / \mathcal{E}_n) + 1 \right]^2}{\sum (1/\mathcal{E}_n)^2 + 1} \right]. \quad (3)$$

The quantity \mathcal{E}_n is the reduced energy and is defined as $\mathcal{E}_n = [2(E_{R_n} - hc/\lambda)/\Gamma_n]$, where E_{R_n} is the energy of the n th resonance. The adjustable parameters q_n , and Γ_n are the shape parameters and the resonance width of the resonance with principal quantum number n , respectively. The background cross section σ_b was chosen to be a polynomial with the same shape as the most recent compilation.⁵ The magnitude of the cross section, however, was an adjustable parameter.

The preceding published wavelength positions⁷ of the resonances (except that of the $2s2p^1P^o$ resonance) converging to the $n=2$ levels of the He^+ were used as wavelength standards to calibrate the wavelength scale of the monochromator. The resonance position of the first $2s2p^1P^o$ resonance was an adjustable parameter.

The width of the resonance quickly became narrow compared to the spectral band of the monochromator, which was about 0.02 eV (0.072 Å). The monochromator bandpass was several times wider than Γ for the higher members of the series. To obtain the fit, shown as the solid line in Fig. 3, to the data for the entire Rydberg series, the cross section was modeled according to Eq. (3). For an unperturbed Rydberg series q_n is constant for the series²⁶ and $\Gamma_n \simeq \text{const}/n^{*3}$. The quantity n^* is the effective quantum number. Thus q_n was set to equal q_3 and Γ_n was set to equal to $21.7 \Gamma_3/n^{*3}$ for $n > 3$. To approximate the behavior of the higher members of the series an arctan dependence²⁹ was added to the expression for the value of the cross section of the Rydberg series given in Eq. (3).

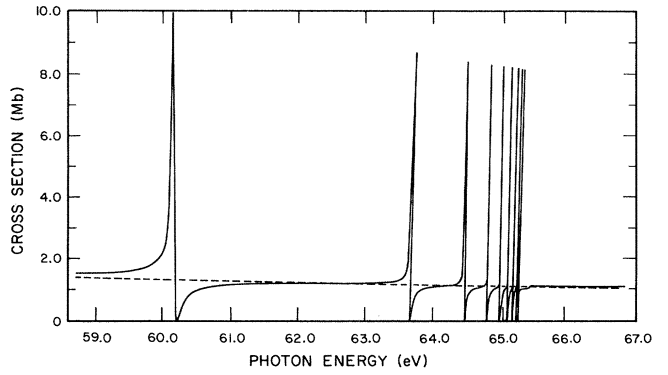


FIG. 3. Helium photoabsorption cross section for the $(sp 2n+)^1P^o$ Rydberg series using parameters from Table I.

IV. RESULTS AND DISCUSSION

Typical transmission for the lowest two-electron excitation state is shown in Fig. 1. The best least-squares fit to the data is shown as the solid line passing through the data points.

Figure 2 illustrates typical transmission data for the Rydberg series. The solid line is the model transmission calculated using the least-squares adjusted parameters. The values of the parameters obtained from this fitting routine are shown in Table I. A comparison of the theoretical and experimental parameters for the $(sp, 2n+)^1P^o$ Rydberg series for levels up to $n=10$ is given in Table II.

A detailed physical interpretation of the asymmetric shape of the resonance in the continuum absorption of helium has been given by Fano.⁶ The quantities q , the asymmetry index, and Γ , the resonance width, have been the subject of several other calculations.^{1,15} The most recent calculation of these parameters is given in the preceding paper of Bhatia and Temkin.²⁴ Figure 4 is a plot of the cross section of $2s2p^1P^o$ resonance obtained using the parameters from Table I. The dashed line is a plot of the energy-dependent background cross section. Figure 3 shows the cross section for the $(sp2n+)^1P^o$ Rydberg

TABLE I. Cross-section parameters for two-electron states in helium.

n	λ^a	n^{*a}	q	Γ (eV)	E (eV)
2	206.21	1.606	-2.6 (± 0.3)	0.038 (± 0.002)	60.151 (± 0.10)
3	194.78	2.791	-2.5 (± 0.5)	0.0083 (± 0.002)	63.655 ^d
4	192.33	3.812	-2.5 ^b	0.0038 ^c	64.466 ^d
5	191.29	4.82	-2.5	0.0014	64.816 ^d
6	190.75	5.82	-2.5	0.0008	64.999 ^d
7	190.43	6.82	-2.5	0.0005	65.108 ^d
8	190.22	7.85	-2.5	0.0003	65.181 ^d
9	190.08	8.85	-2.5	0.0002	65.229 ^d
10	189.98	9.90	-2.5	0.0001	65.263 ^d

^aData from Ref. 7.

^bValue of q held constant for $n \geq 4$.

^c Γ_n is inversely proportional to n^{*3} for $n \geq 4$.

^dObtained from Ref. 7 using 12 398.52 to convert from Å to eV.

TABLE II. Comparison of the theoretical resonance parameters.

State	Propin ^a		Lipsky <i>et al.</i> ^b		Burke and Taylor ^c		Drake and Dalgano ^d		Altick and Moore ^e			Burke and McVicar ^f		
	E^i	E	E	Γ^i	E	Γ	E	Γ	E	Γ	q	E	Γ	q
$2s2p$	60.4	60.2744	60.149	0.0388	60.133	0.0366	60.340	0.0365	-2.97	60.269	0.0438	-2.59		
$2sp,23^k$		63.6879					63.707	0.0070	-2.89	63.690	0.0087	-2.44		
$2sp,24^k$		64.4786					64.537	0.0051	-2.81	64.481	0.0037	-2.42		
$2sp,25^k$		64.49												
$2sp,26^k$		64.8218												
$2sp,27^k$														
$2sp,28^k$														
$2sp,29^k$														
$2sp,210^k$														

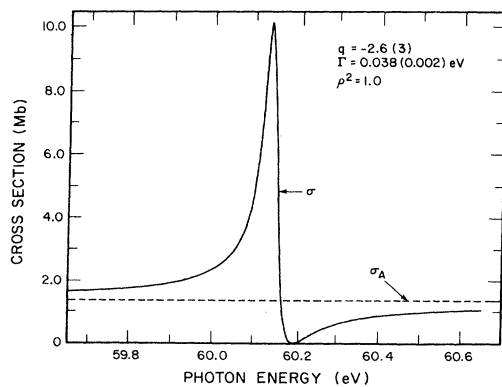
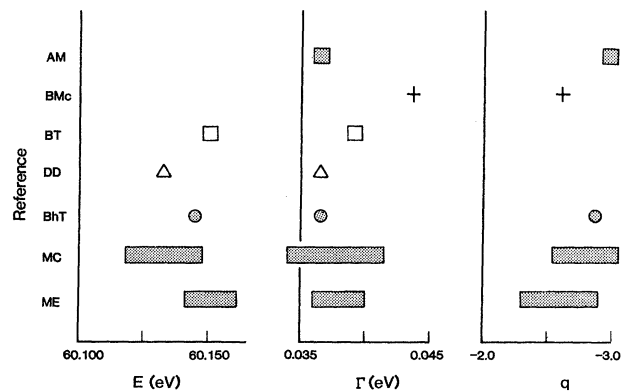
^aReference 11.^bReference 18.^cReference 13.^dReference 16.^eReference 15.^fReference 1.^gReference 24.^hReference 7.ⁱThe quantities E and Γ are expressed in eV.^jThe energy quoted by MC is that for the absorption maximum. This is the MC number scaled to the resonance energy. The quantity of 12 398.52 was used to convert wavelength to eV.^kResonances with principal quantum number ≥ 4 normalized to the value of Ref. 7.FIG. 4. Helium photoabsorption cross section for the two-electron excitation state, $2s2p \ ^1P^0$ using parameters from Table I.FIG. 5. Graphic comparison of the resonance profile parameters E , q , and Γ for the $2s2p \ ^1P^0$ state. The authors are identified by the symbols and the initials along the ordinate as follows: AM (■), Ref. 15; BMc (+), Ref. 1; BT (□), Ref. 13; DD (△), Ref. 16; BhT (○), Ref. 24; MC, Ref. 7; ME, present results.

TABLE II. (Continued.)

E	Bhatia and Temkin ^g		E	Madden and Codling ^h		E	This work	
	Γ	q		Γ	q		Γ	q
60.145	0.0363	-2.849	60.133 ^j	0.038	-2.80	60.151	0.38	-2.6
			± 0.015	± 0.004	± 0.25	± 0.010	± 0.002	± 0.30
63.6610	0.009	-2.6	63.655	0.008	-2.0	63.655	0.0083	-2.5
			± 0.007	± 0.004	± 1.0	± 0.010	± 0.002	± 0.50
			64.466			64.466	0.0038	-2.5
			± 0.007					
			64.816			64.816	0.0014	-2.5
			± 0.007					
			64.999			64.999	0.0008	-2.5
			± 0.007					
			65.108			65.108	0.0005	-2.5
			± 0.007					
			65.181			65.181	0.0003	-2.5
			± 0.007					
			65.229			65.229	0.0002	-2.5
			± 0.007					
			65.263			65.263	0.0001	-2.5

series for levels up to $n = 10$, calculated using Eq. (3) and the parameters obtained from Table I. The dashed line is the plot of the energy-dependent background cross section expressed in Mb ($1 \text{ Mb} = 10^{-18} \text{ cm}^2$) which is given by the equation

$$\sigma(\lambda) = -0.05504 - 1.3624 \times 10^{-4} \lambda + 3.3822 \times 10^{-5} \lambda^2, \quad (4)$$

where λ is the wavelength in angstrom units. This analytical expression can be used to calculate the background cross section between 65 and 280 Å and agrees to within $\pm 2\%$ with the recent compilation⁵ of the helium cross section.

In Fig. 5 the profile parameters q , E_r , and Γ for the $2s2p^1P^o$ resonance obtained from the present measurements (ME) are compared with those obtained by Madden and Codling (MC) and the available calculations, which are identified by symbol and by the author's initials along the ordinate. The calculated resonant energy of AM (Ref. 15) and BMc (Ref. 1) lie outside of the plotted range. The authors DD (Ref. 16) and BI (Ref. 13) did not calculate the value of the parameter q .

The values of the parameters obtained from the experiments are in general consistent with the calculations. However, there are trends which we now discuss. The resonance energy obtained from the calculations of BT (Ref. 13), and DD (Ref. 16) seem to be converging to a value of nearly 60.145 eV, which is the value originally obtained by

BhT (Ref. 24) using a more sophisticated Hylleraas calculation. All the calculated widths except that of BMc lie within the quoted error limits of the experiments. The experiments suggest that the calculated width is somewhat narrow. The quantity q is the most difficult one to measure and to calculate. The experiments and calculations do overlap satisfactorily, but with a larger variation in the value of q , which reflects the difficulty of either measuring or calculating q . The calculations suggest that -2.8 is a reasonable value; however, the experimental evidence may indicate a lower value of q is more appropriate. Of all the calculations, only those of BhT (Ref. 24) lie within the experimental error limits for all three quantities.

In all the calculations that produced a value for q , the magnitude of this parameter decreased for higher series members. This decrease was also observed in both experiment as well (see Table II). For $n > 4$ our data is consistent with a model for which q_n is a constant and for which Γ_n is proportional to the reciprocal of n^{*3} (see Table I and Fig. 2). The result is also reasonably consistent with the results in Refs. 1 and 15.

ACKNOWLEDGMENTS

The authors would like to thank R. P. Madden for his encouragement and the staff of SURF-II for their dedicated service.

- ¹P. G. Burke and D. D. McVicar, Proc. Phys. Soc. London **86**, 989 (1965).
- ²T. Ishinara and R. T. Poe, Phys. Rev. A **6**, 116 (1972); V. L. Jacobs, Phys. Rev. A **3**, 289 (1971).
- ³D. R. Herrick and N. E. Kellman, Phys. Rev. A **21**, 418 (1980). For a more recent review see U. Fano, Rep. Prog. Phys. **46**, 97 (1983).
- ⁴Further summary of the calculations of the total cross section can be found in P. G. Burke, *Atomic Processes and Applications*, edited by P. G. Burke and B. L. Moiseiwitch (North-Holland, Amsterdam, 1976), p. 200; M. Ya. Amusia, N. A. Cherepkov, V. Radojevic, and D. Zivanovic, J. Phys. B **9**, L469 (1976).
- ⁵Measurements of the total absorption cross section are summarized in G. V. Marr, J. Phys. B **11**, L12 (1978); J. B. West and G. V. Marr, Proc. R. Soc. London, Ser. A **349**, 397 (1976) and references therein.
- ⁶U. Fano, Phys. Rev. **124**, 1866 (1961).
- ⁷R. P. Madden and K. Codling, Astrophys. J. **141**, 364 (1965).
- ⁸F. Willeumier, M. Y. Adam, N. Sander, and V. Schmidt, J. Phys. (Paris) Lett. **41**, L373 (1980); D. W. Lindle (private communication).
- ⁹P. Dhez and D. L. Ederer, J. Phys. B **6**, L59 (1973).
- ¹⁰P. R. Woodruff and J. A. R. Samson, Phys. Rev. Lett. **45**, 110 (1980); Phys. Rev. **25**, 848 (1982).
- ¹¹R. K. Propin, Opt. Spectrosc. **8**, 158 (1960).
- ¹²P. G. Burke, D. D. McVicar, and K. Smith, Phys. Rev. Lett. **11**, 559 (1963); **12**, 215 (1964).
- ¹³P. G. Burke and A. J. Taylor, Proc. Phys. Soc. London **88**, 549 (1966); P. G. Burke, in *Invited Papers of the Fifth International Conference on the Physics of Electronic and Atomic Collisions, Leningrad, 1967*, edited by L. Branscomb (University of Colorado, Boulder, 1968), p. 128.
- ¹⁴T. F. O'Malley and S. Geltman, Phys. Rev. A **137**, 1344 (1965).
- ¹⁵P. L. Altick and E. N. Moore, Proc. Phys. Soc. London **92**, 853 (1967); Phys. Rev. **147**, 59 (1966).
- ¹⁶G. W. F. Drake and A. Dalgarno, Proc. R. Soc. London, Ser. A **320**, 549 (1971).
- ¹⁷K. T. Chung and I. Chen, Phys. Rev. Lett. **28**, 783 (1972).
- ¹⁸L. Lipsky, R. Anania, and M. J. Conneely, At. Data Nucl. Data Tables **20**, 127 (1977).
- ¹⁹A. K. Bhatia, A. Temkin, and T. F. Perkins, Phys. Rev. **153**, 177 (1967).
- ²⁰A. K. Bhatia and A. Temkin, Phys. Rev. **182**, 15 (1969).
- ²¹A. K. Bhatia, P. G. Burke, and A. Temkin, Phys. Rev. A **8**, 12 (1973); **10**, 459(E) (1974).
- ²²A. K. Bhatia and A. Temkin, Phys. Rev. A **8**, 1284 (1973); **10**, 458(E) (1974).
- ²³A. K. Bhatia and A. Temkin, Phys. Rev. A **11**, 2018 (1975).
- ²⁴A. K. Bhatia and A. Temkin, preceding paper, Phys. Rev. A **29**, 1895 (1984).
- ²⁵R. P. Madden, D. L. Ederer, and K. Codling, Appl. Opt. **6**, 31 (1967).
- ²⁶U. Fano and J. Cooper, Phys. Rev. **137A**, 1364 (1965).
- ²⁷D. L. Ederer, Appl. Opt. **8**, 2315 (1969).
- ²⁸D. W. Marquardt, J. Soc. Ind. Appl. Math. **11**, 431 (1963).
- ²⁹T. Watanabe, Phys. Rev. **139**, 1747 (1965).